The design of ERIS for the VLT

P. Amico*[1a], E. Marchetti[a], F. Pedichini[b], A. Baruffolo[c], B. Delabre[a], M. Duchateau[a], M. Ekinci[a], D. Fantinel[c], E. Fedrigo[a], G. Finger[a], C. Frank[a], R. Hofmann[d], P. Jolley[a], J. L. Lizon[a], M. Le Louarn[a], P-Y Madec[a], C. Soenke[a], H. Weisz[e].

[a]European Southern Observatory, Karl-Scharzschildstr. 2, D-85748 Garching, Germany
[b]Osservatorio Astronomico di Roma, INAF, via di Frascati 33, I-00040 Monteporzio Catone, Italy
[c]Osservatorio Astronomico di Padova, INAF, Vicolo dell'Osservatorio 5, I - 35122 Padova, Italy
[d]Max-Planck-Institut für extraterrestrische Physik, Giessenbachstraße, D-85748 Garching, Germany
[e]Ing.-Bureau für den Maschinenbau, Menzingerstraße 1, D-80638 München, Germany

ABSTRACT

The Enhanced Resolution Imager and Spectrograph (ERIS) is the next-generation instrument planned for the Very Large Telescope (VLT) and the Adaptive Optics Facility (AOF)[1]. It is an AO assisted instrument that will make use of the Deformable Secondary Mirror and the new Laser Guide Star Facility (4LGSF), and it is designed for the Cassegrain focus of the telescope UT4. The project just concluded its conceptual design phase and is awaiting formal approval to continue to the next phase. ERIS will offer 1-5 μm imaging and 1-2.5 μm integral field spectroscopic capabilities with high Strehl performance. As such it will replace, with much improved single conjugated AO correction, the most scientifically important and popular observing capabilities currently offered by NACO[2] (diffraction limited imaging in J-M band, Sparse Aperture Masking and APP coronagraphy) and by SINFONI[3], whose instrumental module, SPIFFI, will be re-used in ERIS. The Cassegrain location and the performance requirements impose challenging demands on the project, from opto-mechanical design to cryogenics to the operational concept. In this paper we describe the baseline design proposed for ERIS and discuss these technical challenges, with particular emphasis on the trade-offs and the novel solutions proposed for building ERIS.

Keywords: VLT, instrumentation, AOF, AO, LGSF, DSM, ERIS.

INTRODUCTION

ERIS is the proposed 1-5 μm instrument for the Cassegrain focus of unit telescope 4 (UT4) at the VLT, the telescope that will be soon equipped with the Adaptive Optics Facility (AOF)[1]. ERIS uses and depends on the AOF infrastructure to perform the AO correction. The ERIS concept maximizes the re-use of existing sub-systems and components. In particular, the AO correction is provided by the AOF Deformable Secondary Mirror (DSM) and the artificial Laser Guide Stars (LGSs) are generated by the 4LGSF system. The wavefront sensor camera detectors are the ones used for GALACSI and GRAAL (the two GLAO systems of the AOF) and the Real-Time Computer (RTC) is a modified version of SPARTA.

In its **baseline** incarnation (Figure 1), ERIS consists of nine main modules (also referred to as "building blocks"):

- The main structure (MS), dimensioned to **integrate** all the other subsystems
- an AO module, AETHER (Ao modulE To acHieve Enhanced Resolution), which provides NGS and LGS wavefront sensing and real—time computing capabilities, and interfaces to the AOF (DSM and 4LGSF); the baseline choice for the NGS WFS is a pyramid WFS which also serves as a low order (LO) WFS to be used with the LGS.
- a new imager, NIX (Near Infrared camera System). NIX provides diffraction limited imaging, sparse aperture masking (SAM) and pupil plane coronagraphy capabilities in the 1-5 μm range (i.e. J-Mp), either in "standard", observing mode or with "pupil tracking" and "burst" (or "cube") readout mode. NIX is a cryogenic instrument and its 2k×2k detector is cooled at 40K by means of a closed cycle cooler (CCC).

*pamico@eso.org

- the existing SPIFFI spectrograph (a.k.a. ERIS-SPIFFI): ERIS-SPIFFI is a version of SPIFFI, the 1-2.5 μm integral field unit currently on-board SINFONI, slightly modified to be integrated into ERIS. Its observing modes are identical to those of SINFONI.
- a calibration unit
- ancillary systems (electronic cabinets, cables, etc) as required: 2 cabinets already serving ERIS-SPIFFI and 2 new ones for the AO module and the camera.

The development of the ERIS baseline concept started with the analysis of the top level requirements (Section 0) derived by the science cases to obtain general guidelines for the design of the assembled instrument using its main building blocks (modules). In this phase, particular attention was given to the selection, via a trade-off, of the concept for the AO module, given the request of upper management to conduct a full exploration of options for wavefront sensing. The performance analysis concentrated on simulations and iterative adjustments of a first design concept for the AETHER module.

The design phase of ERIS, starting with the optical and mechanical studies, included several other trade-offs (Section 0) and concentrated in producing an instrument concept of proven technical feasibility, which can be fully interfaced to the VLT environment. The system analysis (Section 0) demonstrates that all the requested "performance TLRs" are fulfilled by the current design of ERIS and identifies the major risks (Section 0)

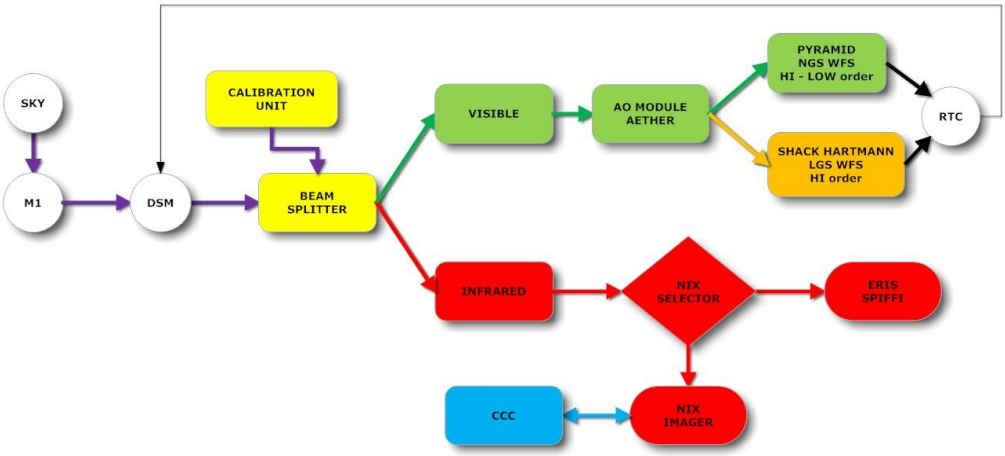

Figure 1: Chart showing the main components of the ERIS baseline design. The shaded boxes are for sub-systems belonging to ERIS, the white ones are external to the instrument.

The conceptual design phase of ERIS (also called Phase A in ESO's terminology) started in 2011, after a trade-off study conducted in-house to select the best option for a new high resolution imager to replace the observing capabilities of NACO, supposed to be decommissioned to free the telescope's Nasmyth focus for the instrument MUSE. The final review and conclusion of Phase A took place on May 24th, 2012 and, at the time of writing, final acceptance is imminent. This event will mark the beginning of the construction phase.

THE PATH TO THE ERIS BASELINE DESIGN: REQUIREMENT ANALYSIS

The requirement analysis phase provided the first step towards the definition of the baseline design of ERIS. Several boundary conditions were imposed from the beginning to the engineering team and significantly restricted the degrees of freedom in the definition of the baseline design. Among those, the two most notable were the re-use of SPIFFI to maintain SINFONI's observing modes with an improved AO performance and the request to study and trade-off different options for wavefront sensing, namely Shack-Hartmann (S-H WFS) and pyramid (PWFS) type of WFSs. While we refer the reader to a specific ERIS AO paper[4] for a detailed description of the AO module, we summarize here the desired basic functionalities. The AO module shall:

- be equipped with **one high order NGS wavefront sensor** for on-axis atmospheric turbulence correction. The number of sub-apertures should be dimensioned in order to fully exploit the DSM correction capabilities guaranteeing high Strehl ratio performance. The WFS FoV shall be dimensioned to efficiently observe up to the requested wavefront sensing source maximum size. Means have to be considered to efficiently sense the requested brightest source.
- be equipped with **one high order LGS wavefront sensor** for on-axis atmospheric turbulence correction. The number of sub-apertures and the FoV should be dimensioned in order to fully exploit the DSM correction capabilities and to cope with the LGS post elongation to guarantee high Strehl ratio performance.
- be equipped with **one low order NGS wavefront sensor** supporting the LGS wavefront sensor to compensate for tip-tilt indetermination due to the LGS use. The number of sub-apertures should be dimensioned to guarantee both the most precise low order correction and the accessibility to the faintest wavefront sensing sources. The WFS FoV is dimensioned to efficiently observe up to the requested wavefront sensing source maximum size. Means have to be considered to efficiently sense the requested brightest source. The NGS searching FoV is dimensioned to achieve the required sky coverage.
- make use of the AOF's **DSM** for correcting the on-axis atmospheric turbulence.
- make use of at least **one laser and launch telescope of the 4LGSF** to generate the LGS wavefront sensing source. The use of additional lasers (and launch telescopes) would be required if the minimum required correction performance from the TLRs is not achieved.
- be designed to minimize the impact of instrumental perturbations (for example flexures) on the correction performance.

The requirements imposed on the imager NIX came from the desire to replace the most scientifically important and/or popular observing modes of NACO, identified in 1-5 μm imaging, pupil plane coronagraphy (PPC) and sparse aperture masking (SAM), making sure to include in the design the lessons learnt in ~10 years of operations. Moreover the imager NIX shall:

- operate in wavelength ranges (K, Lp and Mp bands) where the thermal emission is already important. This in turns sets constraints on the operating temperatures of the optics (80K with a stability of +/- 1K), which in turn implies a cryogenic design.
- include optical elements made of a suitable material and A/R coated to allow transmission or reflection of the light in the 1-5.4 μm wavelength range, and in particular shall be optimized for the 1-2.5 μm wavelength range.
- be designed with a fixed pupil plane for all scales to accommodate the pupil plane masks for SAM and PPC.
- be able to interface to the DSM to support M-band chopping observations in both LGS and NGS mode.
- Have a detector sensitive in the 1-5.4 μm wavelength range, and selected according to the following constraints:
    1. (DC noise) < 0.3 (total noise); in the case of detector with a 5.4 μm cut-off wavelength this requirement, together with the desired cosmetic quality and the characteristics of the science filters (e.g. bandpass), set a constraint on the cooling temperature.
    2. Operations in L (possibly) and M (surely) bands require the capability of fast read-out for both the detector and the associated electronic boards. In case the detector cannot be read at a rate which is shorter than the saturation exposure time for M-band, on-chip windowing capabilities will be needed.
- have at least two filter wheels, one (wheel 1) for filters and the other (wheel 2) on the pupil plane for filters, sparse aperture masks (numbers TBD, in NACO there are 5) and for a pupil plane coronagraphy plate (1 plate); wheel 1 shall be located farther from the detector and shall host the filters needed for SAM and pupil plane coronagraphy. Each filter wheel shall have a minimum of 16 slots, for a total of 32; one of each shall be empty.
- be designed to have pixels scales of 13 mas/pixel (1-2.5 μm) and 27 mas/pixel (1-5.4 μm). This sets a constraint on the combination of pixel size and focal length of the cameras.
- NIX optics shall have maximum one-axis optical distortion σ_s<1.5mas over a 5 arcsec radius, corresponding to 0.150 mas after third order polynomial correction.

For the spectrograph, ERIS-SPIFFI, the requirements are mainly imposed by the need to fully integrate an existing instrument in ERIS, to minimize, mostly for reasons of cost and schedule, the changes (i.e. introduction of novelties) and to at least maintain or improve SPIFFI's performance on sky, in particular on-sky overheads and overall throughput. This last requirement has implication on the need to optimize the ERIS common path optical elements in the SPIFFI wavelength range (1-2.5 μm), given the well-known problem of finding A/R coatings with constant, high transmission over the full 1-5 μm range. The baseline design for ERIS-SPIFFI includes only "upgrades" (to the old SPIFFI) made mandatory by the integration into ERIS. Some other modifications were proposed and are discussed in section 0.

Finally, concerning ERIS as whole system, it shall:

- include optical elements made of a suitable material and A/R coated to allow transmission or reflection of the light in the 1-5.4 μm wavelength range, and in particular shall be optimized for the 1-2.5 μm wavelength range (see the above remarks on ERIS-SPIFFI's throughput).
- ERIS' optics, in particular the dichroic beamsplitter and the selector unit, and NIX's optics, from the entrance window to the detector, shall be designed so that the transmitted unvignetted FoV to NIX has a diameter of 45" or larger. This requirement has an impact in specifying the FoV transmitted to ERIS-SPIFFI: its science field at its maximum, 8"×8", is included in the 45". However, this requirement does not take into account the possible use of the sky-spider (currently not offered with SINFONI) which facilitates simultaneous observations of a blank sky field. The observer may choose one of three fields, with separations of about 15", 30" and 45" from the centre of the SPIFFI field of view.
- The total emissivity from the telescope (excluding M1 and M2) to the last warm surface of NIX in the 1-5 μm wavelength range shall be smaller than 50% of the sum of the atmosphere and telescope emissivity, as published for Paranal.
- ERIS shall be served by a calibration unit providing:
    - A uniformly illuminated image which covers the maximum field of view of NIX once injected in the optical path.
    - one light source, spectrally flat across the wavelength range 0.45-2.5 μm (e.g. Halogen) and of adjustable intensity;
    - Argon, Krypton, Xenon and Neon adjustable intensity light sources to provide spectral lines in the 1.0-2.5 μm wavelength range;
    - a fiber providing a diffraction limited point source image in the 0.45-2.5μm wavelength range, movable in three (x,y,z) axes in such a way to cover at least a 8×8 arcsec field in x and y and ±X (TBD) mm along the z (focus) axis. For the PSF calibration the fiber shall illuminate the whole aperture of the AO module homogeneously.

In designing the general layout of the instrument one shall also consider that:

1) the constraints imposed to Cassegrain instruments at the VLT: the volume envelope at the Cassegrain for a rotating instrument is 4400×4400 mm, the mass limit is 2500Kg and the torque limits are 20kN×m $\perp$ to the optical axis and 500 N×m $/\!/$ to the optical axis.

2) The constraints imposed by the TLRs and by "common sense" considerations on economy of design, minimization of optical surfaces (to increase throughput), of moving parts (to minimize flexures) and the number of cameras on board (which affects mass, torque, volume and power budgets):
    - The calibration unit must serve all sub-systems, therefore its light must be inserted upstream in the optical path before anything else. The simplest solution is to locate the unit on the upper part of the MS.
    - SPIFFI has a preferred operating orientation, with its entrance window looking up at zenith. Therefore it is reasonable to mount it on the lower part of the MS orthogonal to the telescope optical axis, in a similar configuration as the current one with SINFONI.
    - SPIFFI's preferred orientation forces the use of a dichroic beamsplitter which transmits the IR light and reflects the VIS light. The simplest solution is to have the AO module located in the upper part of the MS, opposite the calibration unit. As a consequence, also NIX's entrance window must be located downstream the AO bench in the optical path.

- SPIFFI's entrance window is located at the edge of the cryostat and it is the dichroic beamsplitter in SINFONI. It is reasonable to maintain the direct light feed of SPIFFI, replacing the current window with a flat glass and positioning the dichroic beamsplitter upstream in the optical path, as part of the AO module and fixed to the AO bench, to serve both SPIFFI and NIX. An alternative solution would be to have for SPIFFI and NIX each a dichroic as entrance window. This solution implies a more complex optical design because the visible reflected light must be relayed to the AO module from both dichroic beamsplitters, with an identical path length. Although this design seemed to be feasible after a coarse analysis, it requires a larger number of optical surfaces, some also moving, and for that reason it was discarded.
- Since some space is required for the AO system, the calibration unit and NIX upstream of ERIS-SPIFFI, the design shall either foresee the telescope focus extraction (similarly as what was done for MUSE) or some relaying optics that shift the telescope focus downwards. The first solution is preferred because of its simplicity of design (less optical elements) even though it may introduce some spherical aberration that will have to be corrected by the optics of NIX and ERIS-SPIFFI. The extraction of the focus imposes a new design for the telescope guider, which will have to be a modified version of that for the Nasmyth B (MUSE), taking into account the differences between Nasmyth and Cassegrain rotator/adaptor.
- Since there is no requirement for using NIX and ERIS-SPIFFI simultaneously, switching between the two instruments requires a movable mirror to be inserted in the optical path. This mirror is considered part of NIX.
- General maintenance rules, requires that the electronic cabinets be easily accessible. In our design this implies that they have to be mounted on the external part of the MS, possibly not stiffly attached to the instruments to avoid transfer of mechanical stress. Another constraint is that the detector controllers must be close to their cameras.

All the requirements above were combined in the ERIS baseline design proposal, shown schematically in Figure 2.

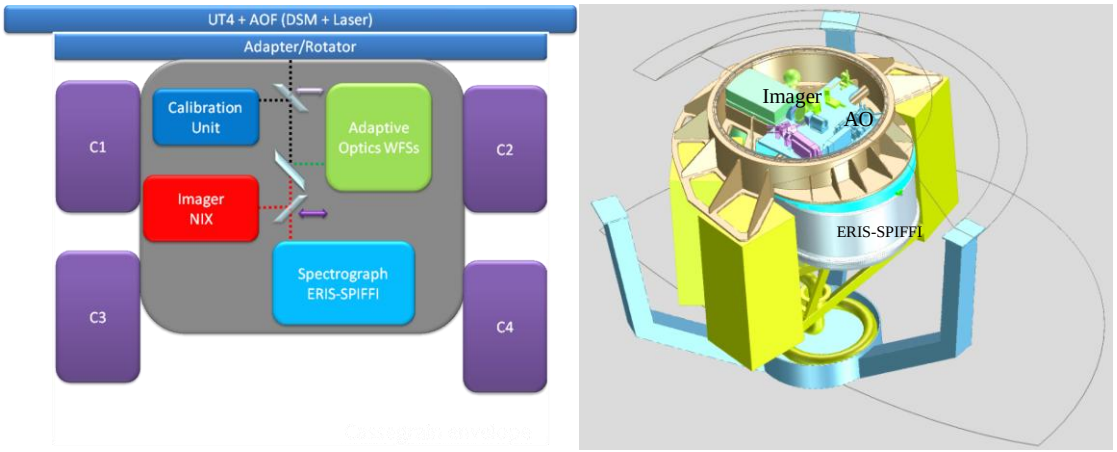

Figure 2. (Left): simple 2-D diagram of the design of ERIS obtained after combining the guidelines discussed in the text. The cabinets (C1-C4) are in reality distributed all around to the MS (not one on top of each other). (Right): Building blocks of ERIS shown in the inclined top-view of the mechanical design.

Note that there is no specific optical design for ERIS since the dichroic is considered part of the AO, the NIX fold mirror is considered part of NIX and the calibration unit fold mirror is considered part of the CU itself.

As mentioned above, the implementation of ERIS requires a modification of the telescope configuration in order to increase the back focal telescope distance from 250 mm to 500 mm.

TECHNICAL TRADE-OFFS

During the design phase alternative options for the sub-systems were considered. Table 1 lists the more important ones, together with the main reasons behind the selection. The details for each are given in the remainder of this section. It is important to mention that all these alternative options were studied and considered feasible. The final selection of the

preferred baseline, which will be the subject of the next study phases, requires input from the project science team, the review board and senior management before consolidation.

Table 1: list of the most important alternative design options which were considered on Phase A and the reason for the selection of the baseline. Details for each of them are given in the referenced sections.

Alternative designs	Options	Reason for choice
Electronic design	1) Baseline 2) Optimized	Cost and schedule
NGS WFS	1) Baseline: PWFS 2) Shack-Hartmann	Performance, request from management
NIX Camera optical design trade-off	1) Baseline: refractive 2) Reflective	Distortion
NIX detector trade-off	1) Baseline: H2RG-Teledyne 2) Orion - Raytheon	Compliancy to TLRs
NIX detector cooling trade-off	1) Baseline: Closed Cycled Cooler (CCC) 2) Pulsed Tube Cooler (PTC)	ESO standards, most difficult to include in the design
SPIFFI upgrades	1) Baseline: only mandatory modifications 2) Recommended, desired and optional modifications	Cost, FTEs, schedule

Electronic design

Two different design options for the on-board electronics have been considered:

1) The baseline design that includes the new components required for NIX and AETHER and introduces no changes to the current SPIFFI electronic design.
2) An optimized design that includes the new components for NIX and AETHER, upgrades some of the SPIFFI components, and proposes an effective solution for volume and weight control, with three standard cabinets + (possibly) a 6-slots NGC instead of 4 cabinets.

The constraints imposed on the electronic design (on-board components) come primarily from:

- The weight, volume and torque requirements but also from
- The desire to follow the announced change in the ESO's standards on control electronics (from VME to PLCs).

For both design options the choice of control electronics for the new subsystems (NIX and AETHER) follows new standards introduced at ESO: the general consensus is to avoid the old ESO standard VME system and its costly CPU board and to replace it with Programmable Logic Controller (PLC) - Component - On-The- Shelves (COTS) - playing the role of Local Controller Unit (LCU) previously allocated to VME unit. Since ERIS is one of the first instruments planning to use this new technology and the one with the most complex functions, there is an additional risk to be taken into account. A preliminary assessment of the novelties imposed by the new standard shows that this risk is to be considered of significant severity and low likelihood.

Baseline vs. optimized electronic design

The design for the on-board electronics includes 4 cabinets, organized by functions (e.g. ICE vs DCE). The ERIS-SPIFFI control electronics is hosted in two of them identical to the ones currently used for SPIFFI. The other two cabinets are reserved for NIX and AETHER, one hosting the controller units + cooling (ICE), the second hosting power supplies, Lakeshore temperature controllers + NGC + cooling (DCE).

There are no operational issues on keeping the current VME-bus based system for ERIS-SPIFFI. On the other hand, the electronic control of NIX and AETHER is based on PLC technology, the standard chosen for new instruments at ESO. The hybrid implementation of technology would make the integration and the maintenance more complex. Weights and volume fit with the allocated budgets, even though the weight distribution is not yet compliant and may require either further optimization and/or a counterweighing mass budget to be added, both of those to be secured in the next project phase.

The optimized design differs from the baseline design in the organization of the cabinets, which now group ICE and DCE functions for the ERIS subsystems, and in some modifications to the ERIS-SPIFFI control electronics. With this

new design, it is possible to eliminate one standard height cabinet, and to implement the recommended upgrades to ERIS-SPIFFI.

The critical aspects being included in the decision matrix between the two options are the layout (linked to weight and volume requirements), the positioning accuracy (linked to the requirement (INS) of maintaining or improving SPIFFI's performance) and the grating wheel encoder resolution (known to be the most demanding hardware item to be upgraded). The motivations for choosing option 1) as baseline design are cost and schedule (i.e. not technical), which are minimized with respect to any other options. This solution is feasible and, although not optimized, it imposes no insurmountable issues. However, were the resources available in the next phases, the choice would be that of option 2).

NGS Wavefront sensor

The High Order NGS WFS considered for the baseline design is the Pyramid WFS. The incoming light is split into four slightly diverging sub-beams by a refractive pyramid. A lens assembly re-images for each beam the telescope pupil (0.960 mm diameter) on the detector. The maximum transmitted FoV is 5 arcsec diameter. A filter wheel in front of the refractive pyramid is supporting different diaphragm to narrow the FoV (down to 1 arcsec TBC) and neutral density filters to dim the light of bright NGS reference sources in order stay within the linearity range of the detector (Neutral Density=1 largely enough for $m_R \sim 0$). Refer to the ERIS AO paper[4] for figures.

The pixels of the detector act as sub-apertures: each pupil is mapped by 40×40 pixels equivalent to 40×40 sub-apertures. The number of sub-apertures can be reduced to 10×10 by binning the detector pixels before reading them out (4×4 binning).

For closed loop operations the image of the NGS reference source is modulated along a circular path around the tip of the refractive pyramid by means of the fast jitter mirror. The amplitude of the modulation is selected by the user according to seeing condition and NGS reference source magnitude. The speed of the modulation is locked to the detector integration time and synchronized by the detector controller: always one full modulation loop per integration time. The maximum detector frame rate is 1200 Hz. The stabilization of the pupil image on the detector is guaranteed by the ancillary loop driving the Pupil stabilization mirror.

Pyramid vs Shack-Hartmann WFS

An alternative to the High Order and Low Order NGS WFS baseline design based on Shack-Hartmann was also considered for a trade-off, given that the S-H for ERIS would be an "easy" copy of one of the WFSs of GRAAL.

Numerical simulations were done to compare the correction performance of the NGS PWFS vs. the SHWFS. Dedicated code has been developed with OCTOPUS, the numerical simulation facility developed by the ESO's AO department. Both high order (40×40 sub-apertures) and low order (2×2 sub-apertures) configurations have been considered for both WFSs.

The NGS High Order wavefront sensing mode has been simulated both with PWFS and SHWFS configuration. Both configurations have 40×40 sub-apertures WFS and make use of the 1170 actuators DSM. The corrections performance has been evaluated in terms of Strehl ratio at 2.2 μm (K band) for different NGS fluxes (here expressed in detected photons/m^2/ms). For each flux the closed loop parameters (loop frequency, gain, weighted centroid of gravity size for SHWFS, etc…) have been optimized to achieve the best possible correction.

The comparison is shown in Figure 3. The PWFS is performing significantly better than SHWFS both at high and low NGS flux. At the bright end the difference is explained by the better rejection of the spatial frequency aliasing of the PWFS w.r.t. the SHWFS. The difference at low fluxes is due to the well known gain of the PWFS which benefits from the full aperture correction seen by the sensor: the NGS PSF gets significantly narrower and sharper on top of the pyramid tip increasing the sensitivity w.r.t. the SHWFS especially for the low spatial frequencies. Under same low flux conditions the PWFS provides a better estimate of the incoming wavefront than the SHWFS. Figure 3 shows a gain of 1.5-2.5 magnitudes (between 4 and 10 times flux gain), a value very similar to the one predicted by theoretical models.
De facto, the PWFS outperforms the SHWFS.

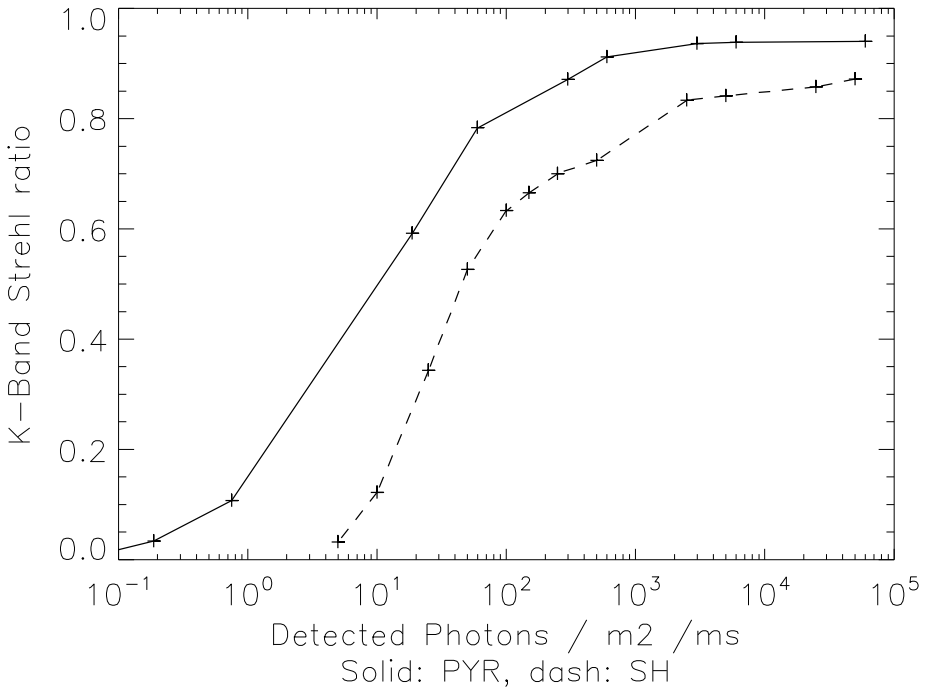

Figure 3. High order NGS PWFS correction performance (solid line): K band on-axis Strehl vs.NGS flux. As comparison the SHWFS performance (same configuration) is shown (dashed line). The error budget is not included. A flux of 10^0 ph/m^2/ms corresponds to a R~17.5 magnitude star.

Low Order WFS

The NGS Low Order wavefront sensor supporting the LGS WFS mode has been simulated both with PWFS and SHWFS configuration. Both configurations have 2×2 sub-apertures, the SHWFS works in almost quad-cell geometry (only the central 2×2 pixels in the sub-aperture are really interested by the NGS PSF, i.e. similar to the PWFS one). In both cases the LGS WFS is 40×40 SHWFS making use of the 1170 actuators DSM. As for the high order WFS, the corrections performance has been evaluated in terms of Strehl ratio at 2.2 μm (K band) for different NGS fluxes (here expressed in detected photons/m^2/ms). For each flux the closed loop parameters (loop frequency, gain, etc…) have been optimized to achieve the best possible correction. The correction performance for the two WFSs does not differ too much, an expected result when taking into account that both sensors resemble a quad-cell geometry for the sub-apertures. Also in this case the PWFS performs better than the SHWFS in a range of low flux conditions but with less gain (up to 1.5 magnitudes) than for the high order case due to the fact that in this case the SHWFS sees an NGS PSF with sharpness similar to the one of the PWFS (just a factor of 2 in resolution). When correction is very poor (very low flux) the noise dominates and the two WFSs provide similar performance.

NIX Camera optical design trade-off

Ideally the optical design of the imager should be diffraction limited, achromatic, include as few components as possible and as few moving parts as possible. Those requirements are best satisfied together by a reflective design, which additionally is ghost-free. The first optical design option for NIX was indeed chosen as a reflective design.

The major drawbacks of this design for the specific case of ERIS were the difficulty to include three wheels (aperture wheel, pupil wheel and filter wheel), which could be solved, and the distortion introduced by the mirrors, around 2%, which was outside the requirement and could not be easily solved. It was decided to switch to a refractive design, which is the current baseline.

The camera has three available re-imaging optics with two different scales as shown in Table 2

Table 2: available camera scales and their main characteristics

Camera	Bands	Scale	Field of view (arc sec)	F/#
1	JHK	13 mas/pixel	26.6 x 26.6	35.7
2	JHK	27 mas/pixel	55.3 x 55.3	17.2
3	LM	27 mas/pixel	55.3 x 55.3	17.2

Two of the requested observing modes for NIX, namely SAM and PPC, require that the pupil position be fixed along the optical path, where the pupil wheel is located. This imposes the use of a movable mirror to compensate for the variation of the focal length between the 13 mas/pix and the 27 mas/pix cameras. The pupil image inside the camera is therefore common to the 3 objectives. Its diameter is 8.6 m and it is also the cold stop of NIX.

The layout of NIX is shown in Figure 4.

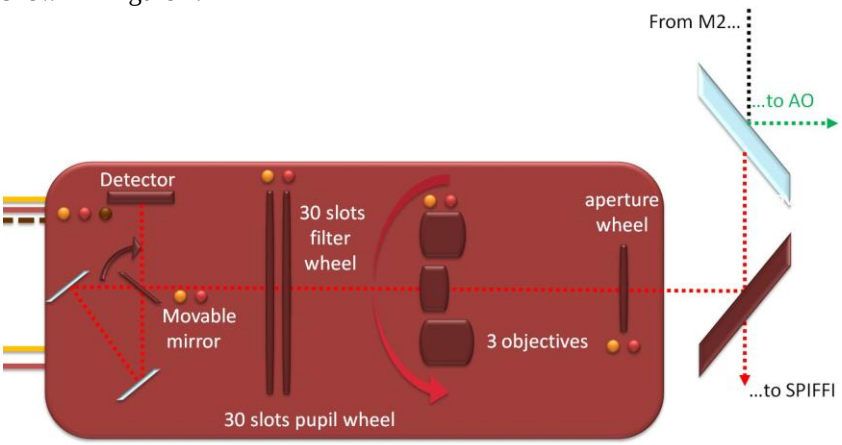

Figure 4: diagram of the imager. It includes five moving cryogenic mechanisms, the aperture wheel, the objectives carousel, the filter and pupil wheels and one selector mirror. The detector is controlled by ESO's New Generation Controller (NGC). The shaded lines indicate the type of interfaces connected to the subsystem. The dotted line indicates the light path.

It includes:

- The **selector mirror** which folds the optical path towards NIX
- The **entrance window**.
- An **aperture wheel** on the telescope focal plane; it contains field diaphragms
- The **camera exchange mechanism**, a wheel that holds the three objectives.
- The **filter wheel**, that holds filters and one empty slot
- The **pupil wheel**, that contains SAM masks, the AP plate, filters and empty slot
- The **movable mirror**, which is inserted when one of the 27 mas/pix cameras in selected.
- The **fixed mirrors (2) assembly** used instead of the movable mirror when the 13 mas/pix camera is selected.
- The **detector**, fixed.

The movable mirror mechanism also hosts a lens assembly, operating from J to K band, that creates the image of the pupil on the detector when inserted in the optical path. It is required for alignment purposes. This lens is a triplet which provides a slightly magnified image of the pupil on the detector (x 1.1)

NIX detector trade-off

Following the requirement analysis discussed in Section 0, we analyzed in more detail the requirements on the detector's parameters. These requirements are summarized in Table 3, where the resulting detector's specifications are shown in bold fonts.

Table 3: TLRs matrix for the selection of the NIX detector

TLR	1- NACO modes	2- Handling warm & cold	3-J to Mp	4- scales mas/pix	5- <1.5mas distortion FOV ∅> 45"	6- Low overhead	7- Dark noise < 30% total noise
1	**Format square** Max. FOV ∅ = 54"			Nyquist sampled ⇓ **Low Crosstalk and linearity > 95%**		Implementation of **Cube Mode**	Most demanding : Jnb @ 13 mas/pix the with bkg= 0.3e/pix/s ⇓ dark < 0.1*bkg ⇓ **Dark< 0.03 e-/pix/s** J bkg = 5e/pix/s ⇓ **Dark < 0.5 e-/pix/s** ⇓ Operative **temperature below 40K** to limit dark current
2		Survive multiple thermal cycles without damages or cosmetic degradation	No warm operations only storage and handling		**Low TEC ($<10^{-5}$)** is requested for astrometry calibration		
3			Spectral coverage from **1.0 to 5.1 μm with Q.E. > 80%**		The Nyquist sampling of PSF reduces **FOV at 13 mas/pix scale**	Most demanding : Mp @ 27 mas/pix due to bkg flux = 1e7 e/pix/s ⇓ Saturation. DIT= FW/1e7 Typical FW= 1e5 ⇓ Saturation DIT=10ms **min DIT ≈ 5ms**	
4				Two different optical magnifications	Detector format > 1670 x 1670 pixels ⇓ **2k×2k good choice**		
5					The use of a 2kx2k detector ⇓ reduced FOV @13 mas/pix		
6						**CMOS architecture, fast readout, low latency and windowing capability**	
7							

The detector trade-off compared Raytheon's Orion InSb with Teledyne's H2RG HgCdTe (5.4 μm cut-off) devices.

From this comparison it is evident that the H2RG fits better than Orion in many of the most critical areas of NIX. The H2RG's lower dark current and noise together with the faster frame rate are the decisive factors.

When one compares the requirements in Table 3 with the H2RG's performance specifications the following considerations can be done:

1) Format, pixel size, wavelength coverage, linearity QE and multiplexer architecture are fulfilled/optimal for NIX
2) Crosstalk is acceptable
3) The average dark current (that is, the conservative value) is adequate, provided that the temperature is below 40K, for the demanding application in J@13mas/pix. The most demanding J_{nb} filter, which is presently not required by science, requires a 40% lower dark current. It should be noted, that Teledyne sets a goal value that is 5× lower than what specified. This implies that even the J_{nb} would be compliant and that higher detector operative temperatures might be used, relaxing the performance demands on cryogenics.

4) The saturation DIT in Mp band is 10ms below the required minimum readout time of 26 ms with the 5MHz fast readout ports (which becomes 70 ms due to the current bandwidth of ESO's detector controller, NGC). This implies that not even the best detector on the market can fulfil the NIX requirement: for a 2k×2k array the readout speed should be ~26MHz or not less than 20MHz if one accepts to relax the full well requirement. The only way to overcome this limit is to read fewer pixels, that is, to observe in windowed mode.

   Assuming that a reasonable level of signal is equal to half of the full well, one can calculate the maximum number of pixels that can be read in ~5 ms. It should be noted that given the configuration of the multiplexer, one gains in speed only when windowing is applied in the vertical dimension (orthogonal to the 32 channel buses). Given a pixel sampling time of 0.5μs (i.e.2MHz) and the use of all 32outputs, the maximum window is 2048×156, corresponding to a FoV of 55"×4.2". Only by relaxing the full well requirement to 80% of saturation one could get a 2048x256 (55"× 6.9"). The possibility to upgrade NGC and obtain faster readouts (up to 5MHz) will have to be investigated in the next project phase. Also in the case of Lp band the full frame cannot be readout, the largest window is ~2048×1024 pixels, 55"×27.5".

   ESO currently has 32 channel 10 MHz ADC board which is already operational with the SAPHIRA 320x256 pixel eAPD array to be installed in GRAVITY. It has to be investigated how fast the fast outputs of the Hawaii-2RG can be operated. If 10 MHz operation is possible, readout times of 13 ms are feasible. It will always come to a trade-off between crosstalk (settling time of the video signal due to finite electronic bandwidth) and speed. At high flux only uncorrelated read-reset on a line by line basis will be used since KTC noise is negligible.
   If this is confirmed it will be possible to increase the size of the sub-windows.

In conclusion, there are no problems of feasibility for what concerns the H2RG, provided that the windowing limitations in Lp and Mp bands are acceptable for the science. However, the 5.4 mm cut-off is a novel detector, and more tests are needed before one can make a full assessment of the performance for NIX. Aside from the above, there are other detector parameters that need to be evaluated, such as cosmetic stability over time and its dependency on temperature, and such as persistence, which is a device dependent feature. Earlier procurement and the availability of a proper in-house testing facility are mandatory requirements for the next phases of the project. It should be noted that the same type of detector is envisioned for the MATISSE instrument at ESO.

NIX Detector cooling trade-off

Following the requirement analysis, two possible design options for the cryogenics have been studied. A standard Closed Cycle Cooler (CCC) was selected as the baseline design and an alternative solution which uses a Pulsed Tube Cooler (PTC) was studied for a trade-off. The first one uses a Gifford Mac Mahon traditional cooler to cool the complete instrument. The second uses a LN2 solution and a pulsed tube to bridge from 77K to 40 K. ERIS is a very high resolution instrument and requires a low vibration environment to maintain its performance: vibrations considerations are also discussed.

Considerations on vibrations

Years of experience with CCCs have shown the difficulties and even the impossibility of building a representative model of the vibrations induced by such devices. On the other hand, measurements with the VLT instrumentation can be used to estimate the impact of the vibration caused by a standard Gifford Mac Mahon CCC head on ERIS.

NACO is currently the only VLT instrument that loses significant performance due to the vibration caused by its own cooler. NACO is still equipped with an old version of gas driven cold head and recent tests have shown that this system cannot be improved and cannot be used for reference. Other tests with a CCC of the same type of ERIS and in a similar Cassegrain configuration showed that the effect of vibrations in the WFE is around ~35 nm, ~ 10× less that those induced by the NACO CCC. This design will therefore not affect the VLT-I and most probably not affect the performance of ERIS, provided that the mounting of the optical component is carefully done. If necessary ERIS can also still be upgraded with an active compensation system from which a prototype has been recently tested successfully on HAWK-I.

Despite these encouraging results, the risk that the vibrations induced by the CCC on ERIS translates into loss of performance is still significant, especially considering that ERIS is required to deliver high SRs and that the effect of vibrations are unpredictable and dependent on the mechanical design, materials, etc. As a consequence, it was proposed an alternative PTC design, which is free from the problem of vibrations. Given that the moving masses are reduced (~300g), it is higher frequency (50Hz) and it is compensated with the two displacers in opposition there will be very little vibration transmitted to the instrument.

CCC vs PTC

Table 4: Comparison between PTC and CCC options. Highlighted in bold the most critical ones.

Parameter	LN2 / PTC design	CCC base line design
Type of cooling	LN2 solution and a pulsed tube to bridge from 77K to 40 K	Traditional cooler to cool the complete instrument
Operation temperature	(-) R&D required for testing ability to reach desired detector temperature and to operate with dynamically changing cryostat orientation.	(+) Large margin
Temperature stability	(-) R&D required to test stability, in particular its dependence from LN2 filling level and cryostat orientation	(+) No problem
Vacuum hold time	(+) Better even in case of power failure or PTC problem since the LN2 will cool the sorption pump.	(-) Uncontrolled situation in case of CCC or power failure
Mass	**(+) 85Kg**	**(-) around 60Kg + weight of helium lines + weight of reinforced cable wrap.**
Cable wrap design	(+) Simpler, because no Helium high pressure lines needed	(-) More complex, since high pressure lines required
Electronic safety	(-) Need to implement interlock to control the cooling flow for safety reasons.	(+) No additional design (ESO standard)
Thermal environment	(-) Need to cool the compressor	(+)
Reliability	**(-) R&D needed to test reliability**	**(+) ESO standard**
Maintenance	(-) Difficult and bad access	(+) ESO Standard, staff trained
Operations	(=) One refilling per day[2]	(=) Nothing excepted one maintenance every 6 years
Vibrations	**(+) Tests required to measure vibrations, although the vibration level is known to be significantly lower**	**(-) Evidences of reduced performance due to vibrations and impact on VLT-I.**

Of the various parameters being considered the most relevant ones for ERIS are:

1) **Total mass** added to the budget: the devices' weight is similar (85kg for PTC and 60kg for CCC) but the CCC option adds the weight of the high pressure lines for Helium and the weight for a reinforced cable wrap.
2) **Reliability**: it is an important factor for Paranal operations and R&D must definitely answer the question whether it is an issue for the PTC option.
3) **Vibrations**: the single most critical parameter for ERIS, because vibrations at various frequencies can significantly affect the final correction performance, especially when the low order NGS reference star is faint and the related control loop runs at a slower frame rate. Note that no vibrations have been included in the AO performance simulations and that the WFE budget also does not explicitly include them and they should fit, together with the image motion due to flexures, within the buffer allocation.

For the ERIS baseline design the CCC was chosen because it is an ESO standard, a well known and verified system and, of the two options, the most difficult one to include in the ERIS design, due to the weight and vibrations constraints. The PTC is a very appealing option, especially for its low vibration characteristics, but it requires R&D activities to test performance, operability and reliability. The fact that it is already being considered for the ESO GRAVITY instrument is

[2] In ERIS this is not critical since the daily refilling is required for ERIS-SPIFFI.

a plus. Additionally, in case of system failure, unlike the CCC, the PTC prevents thermal shocks to the detector thanks to the thermal link to the LN2 vessel.

A final trade-off between the two systems is not possible with the available information but it will be a pre-requisite for the final design because switching from CCC to PTC implies significant design changes.

SPIFFI upgrades

Compared to the current SINFONI the differences are: 1) no optical elements before the beamsplitter, as opposed to the 5 mirrors design of SINFONI; 2) Insertion of a flat entrance window to SPIFFI. In SINFONI this function is covered by the beamsplitter; 3) Replacement of the fore-optics collimator (3 lenses instead of 2).

Several considerations have been taken into account for the modifications to SPIFFI. Aside from those mentioned in section 0, the following were included:

1. It is considered that by the time ERIS will be on-sky, the SPIFFI hardware will be already 10+ years old. Although presently there are no major failures or concerns, it is reasonable to assume that with time the hardware will suffer from increased failure rate and gradual obsolescence of its components; in the meantime the ESO standards will have already changed. Experience recommends considering hardware upgrades to those functions of SPIFFI which are subject to wear.
2. In order to economize on the total weight it is recommended to modify the baseline electronic design as discussed in section 0 minimizing the total number of electronic racks, which in turn imposes porting the electronics of SPIFFI to PLCs.
3. It is considered that upgrades to existing functionalities may benefit the scientific output and the operational efficiency of the instrument and as such their implementation is recommended.
4. It is recognized that the improved AO performance of ERIS might make new science cases within reach of the instrument and therefore a list of desirable, optional new functionalities were discussed.

A summary of the proposed upgrades is given in Table 5.

Table 5: Changes considered for the upgrade proposal: mandatory, recommended, desirable, possible.

	Upgrade type	Reason
Mandatory	Replacement of the entrance window	Design change
	Replacement of the fore-optics collimator	Change of F/#
	Modification of the cryostat lid	Background limitation
	Modifications of the sky-spider	Change of entrance pupil
	Replacement of the grating drive	Repair, efficiency
Recommended	Replacement of the motors, use of PLCs and NGC, new electronic design	Weight budget, new standards, resolve obsolescence
	Replacement of the J-band filter	Increase throughput
	Replacement of all pre-optics with better J-band transmission AR coatings	Increase throughput
	Replacement of the detector	Performance, persistence
Desirable	Replacement of the SPIFFI cover plate	Weight budget
	Commissioning of the sky spider	On-sky efficiency
	Upgrade with a higher resolution R~10.000 K-band grating	New science
	Upgrade sky-spider with a coronagraphic mask	New science
	Replacement of the sky-spider with a focal plane unit of choice, e.g. providing polarizers, coronagraphic masks	New science
Possible	Replacement of the spectrometer optics (mirrors)	Better line shapes and resolution

SYSTEM ANALYSIS

The baseline design was finally analyzed to identify possible non-compliances with the requirements. In the case of NIX, for instance:

Mass budget: the preliminary mass budget shows that ERIS already is at the maximum allowed mass without contingency. In the current project phase the mass estimates are coarse and therefore we consider this issue as a potential high risk to be monitored in the next phases. However, all things remaining the same, we estimate that the mechanical design can be optimized to gain some margin: ~15% reduction of weight can be achieved by 1) optimizing the structure and the mechanical design in general (~200Kg less) and 2) by adopting the new electronic design.

Throughput budget: for all the optical components belonging to ERIS we have used values of transmission for research quality material that is a standard for scientific instruments. The dichroic beam splitter and the NIX entrance window are the only two components that must transmit the whole wavelength range (1-5 μm), and this limits the performance that can be achieved even with custom A/R coatings. Following the requirements, we optimized the transmission for J-K (98%). On the other hand, the lenses in the camera's objective transmit each either J to K or L to M and achieve a better performance (99%). For the mirrors an average reflection of 99% was used. Filters transmission were derived from published data of current IR instrument at ESO. The detector QE is the published value of the H2RG. Table 6 reports the estimated throughputs.

Table 6: estimated throughput of the system (atmosphere to detector), of ERIS, of NIX (cold optics only)

	JHK 13 mas	JHK 27 mas	LM 27 mas	Note
Throughput [%]	42	42	41	Atmosphere to detector
ERIS [%]	60	60	57	Dichroic to detector
Cold Optics NIX [%]	81	81	81	No detector

Emissivity budget: emissivity calculations were performed for the available NIX setups JHK/13-mas/pix and J-M/27-mas/pix. Additional setups for J-NB and L-NB filters were included. The assumed ambient temperature is 285 K. (12°C). Figure 5 shows the resulting added background as a function of the filter.

Distortion analysis: the optical distortions calculated from the available optical models for the JHK-13mas/pix and the LM-27mas/pix cameras give the percentage of distortion as a function of the radial distance from the optical axis. The typical maximum distortion (at the edge of the field) is below 0.06%. This value can be further improved by applying a third order polynomial correction that leaves an uncorrected distortion well below 150 μas.

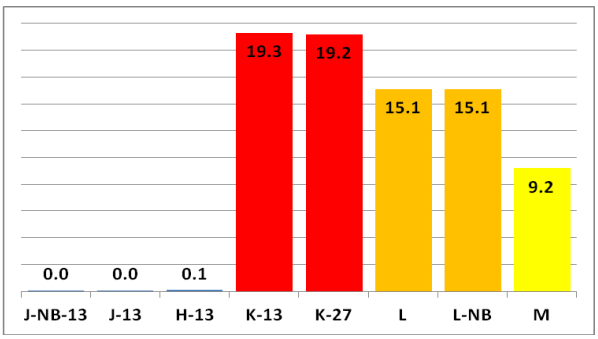

Figure 5: Added background [%] versus band.

Signal to Noise and Limiting magnitude analysis: for a final comparison of the camera performance as a function of different setups, we calculated the achievable limiting magnitude as a function of the exposure time for different detector setups and instrument performance in the band of reference (Figure 6). The conclusions that can be drawn are: the limit magnitude is independent of temperature from J to Mp, and in J_{nb} the limit magnitude the maximum loss is ~1 magnitude. It should be noted that the S/N for long exposures decreases as a function of the detector temperature of ~ 1 unit and that the S/N in J_{nb} is significantly affected by the detector temperature (~50%). The higher temperature of the

detector induces worse cosmetics, which in turns affects the noise histogram. This means that the values of achievable values of S/N and limit magnitude could change for the worse at shorter wavelengths: we calculated that, for instance, in J band the limiting magnitude worsen by less than 0.2 magnitudes when the RON is tripled for the 77K setup.

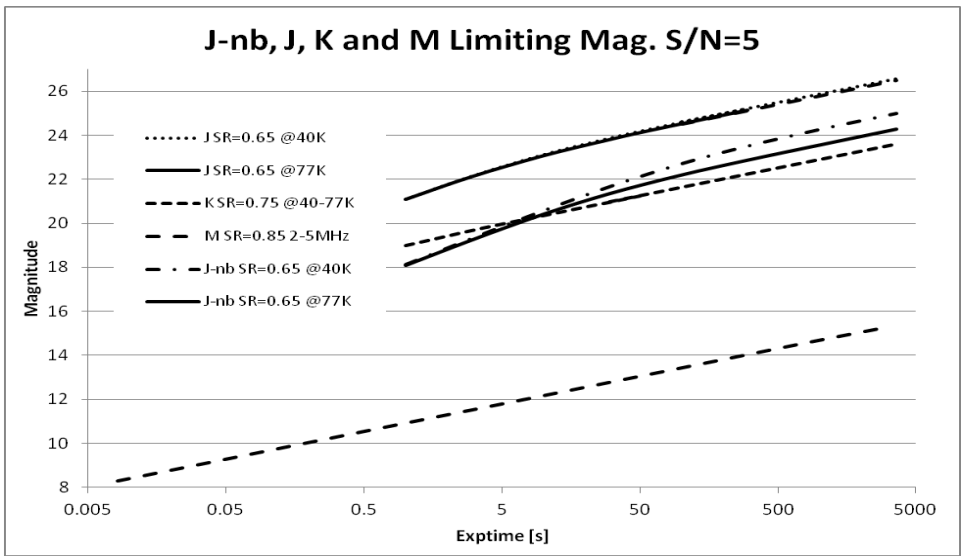

Figure 6: Limiting magnitude as a function of exposure time for J_{nb} and J both at 40 and 77K, K and M band.

Finally we computed the effect on achievable limit magnitude as a function of Strehl (Figure 7).

From the overall analysis one can conclude that the SR has the biggest impact on scientific performance. Detector performance (RON, cosmetics, dark current) has no or very little effect in the J-Mp bands, but they affect J_{nb}. Before the next project phase the science will have to guide the engineering team in selecting the most appropriate choice as a function of the desired scientific outcome. Concerning the detector's cooling, it was decided to keep the baseline design of CCC or PTC with the goal of reaching 40K. However, the 77K option remains competitive except for J_{nb} and for this reason we consider it an acceptable backup solution were the proposed cooling options not implementable.

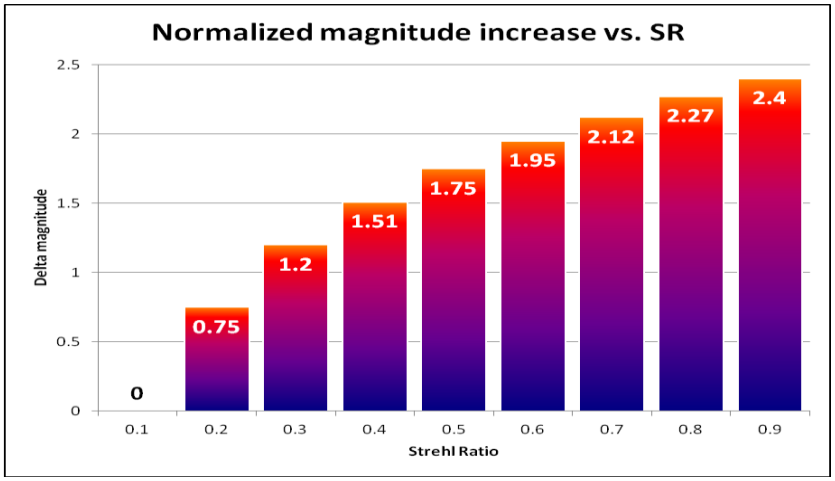

Figure 7: Limit magnitude gain, normalized to limit magnitude at minimum Strehl (0.1) as a function of SR. The data are common to all wavebands.

Flexure analysis: the flexures for the centers of gravity of NIX and the WFS system were calculated for telescope elevations 0 (horizon), 30, 60 and 90 (zenith) and for 4 different rotator angles (0, 90, 180, 270). These calculations do

not include flexures within the components. i.e. the subsystems are considered as rigid bodies preserving their optical properties (e.g. focal length, magnification and distortions). We calculated the displacements and tilts of the instrument optical axis as a function of the differential linear and angular offsets of the center of gravity (CoG) of the instrument, relative to the CoG of the AO bench. In this way it was possible to simulate and analyze the path of the centroid of a tracked optical source on the detector field as a function of elevation and rotator angle. It was assumed that the AO module is controlling the tracking and therefore that the effects are only generated by the differential flexures between NIX and the AO bench, both supposed as rigid bodies.
The typical NIX science exposure is 60-120 seconds long in broad band imaging mode and ~10-15 minutes in narrow band. Table 7 lists some typical science objects observed for 60 minutes in different positions, the typical drifts speed of the optical axis and the exposure time to blur the images for more than 1/20th of a pixel (13 mas/pix scale) as determined using graphs of the type of Figure 8.

Table 7: Observational parameters of typical targets and approximate drift speeds in μas/min. Pixel scale is 13 mas/pix.

Target	Elevation start [degrees]	Elevation increment [degrees]	Rotator start [degrees]	Rotator change [degrees]	Optical axis drift speed [μas/min]	Time to 1/20 pixel drift [min]
Galactic center	80	6	302	117	10	> 60
Galactic center	54	12	267	7	8	> 60
NGC 7582	70	3	342	44	8	> 60
Betelgeuse	57	1	190	25	12	54
Zenith +3	55	13	266	8	14	46
Zenith +3	84	3	293	133	12	54

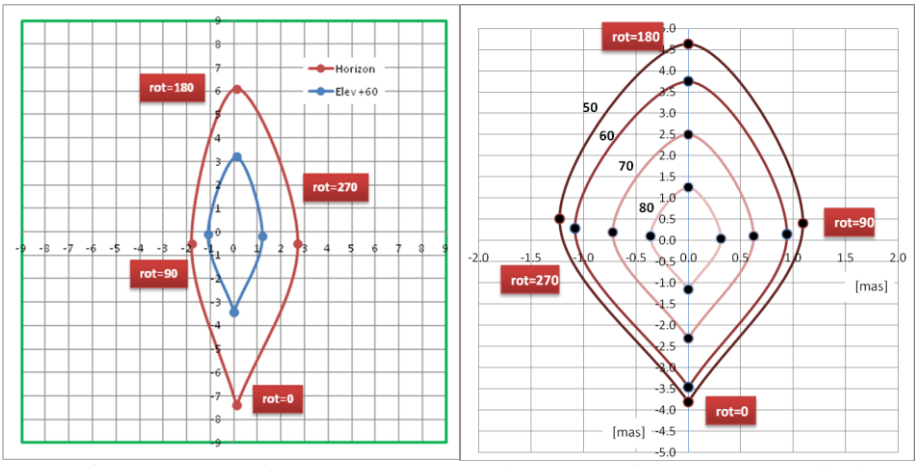

Figure 8: (Left): path of the projection of the optical axis on the focal plane of NIX as a result of a full rotator turn. The outer square is the same size of one pixel (13mas/18 μm) The external curve represent the case of telescope at horizon (worst) and the internal line the case at elevation=+60 (typical of astronomical observations with AO). (Right): path of the projection of the optical axis on the focal plane of NIX as a result of a full rotator turn for elevations of 50. 60, 70, 80 degrees, typical for AO observations. Note that the axes scales are different and in [mas]. This graph can be used to evaluate the maximum smearing of the PSF due to flexures during tracking.

Image quality budget: The image quality budget (see ERIS AO paper[4]) allocates 32.3 mas of image motion in the NGS case and 36.1 mas in LGS, for a typical exposure of 15 minutes.

For each element in the optical path of ERIS it was possible to evaluate the effects of shifts and rotations on the focal plane, typically using conservative values. We finally compared these values with the available budget. From the flexure analysis we estimated that the maximum effect due to differential flexure between NIX and WFS during a typical astronomical exposure (Table 7) of 15 minutes is ~0.42 mas, taken from the worst case multiplied by a safety factor of 2.

We assigned a budget to the different subcomponents tilts and shifts and calculated the total displacement in [mas] at the focal plane, assuming a ~3:2 share between tilt (most sensitive) and shift.

In the most pessimistic case, the effects of the shifts and rotations are added linearly and give a total displacement of the optical axis at the focal lane of NIX of 34.3 mas. In the standard evaluation, the same effects are added quadratically and give a total displacement of 32.7. From this analysis we derived the specifications for the opto-mechanical sub-components of ERIS:

1. Tilt < 1mDeg=3.6". The radius of the fold mirror is approximately 40mm, the radius of the dichroic, 50mm. It results that one mDeg of rotation around the component's barycentre corresponds to 0.7 μm shift at the edges for the fold mirror and 0.9 μm for the dichroic.
2. Shift <4μm.

The pessimistic case suggests that these quantities should be ~halved to be on the safe side.

RISK TABLE

Table 8 lists the risks identified by the project team during the phase A.

Table 8: summary of the identified risks for ERIS

Risk	Severity	Likelihood
Electronic design: use of new PLCs standard	Significant	Low
PWFS		
Know-how	Low	High
Calibrations	Low	High
Sparta modifications	No risk	High
Lack of testing facilities	Low	High
CCC – Vibrations	Critical	High
Mass budget	Critical	Medium-High
Volume budget	Critical	Medium-Low
Torque budget	Critical	Medium
Differential Flexures		
Dichroic	Critical	High
Selector Mirror	Critical	High
Internal flexures AETHER	Critical	Medium
Internal flexures NIX	Critical	Medium
Internal Flexures ERIS-SPIFFI	Critical	Low

CONCLUSIONS

We presented the results of the design phase of ERIS, the next-generation instrument planned for the Very Large Telescope (VLT) and the Adaptive Optics Facility (AOF). We discussed the genesis of the baseline design from a set of scientific and boundary requirements imposed to the project. The major trade-offs between feasible alternative designs options were discussed together with the related technical challenges. The system analysis shows that design is feasible and that the areas of risk were identified. Those will form the base for the beginning of the construction phase, pending approval.

REFERENCES

[1] Arsenault, R. et al, "ESO adaptive optics facility", SPIE Proc. 7015 (2008)
[2] NACO website: http://www.eso.org/sci/facilities/paranal/instruments/naco/index.html
[3] SINFONI Website: http://www.eso.org/sci/facilities/paranal/instruments/sinfoni/overview.html
[4] Marchetti, E. et al, "ERIS Adaptive Optics System design", SPIE Proc. 8447 (2012)